Journal of Sustainable Development of Energy, Water and Environment Systems

http://www.sdewes.org/jsdewes

Year 2018, Volume 6, Issue 1, pp 129-149

Technical and Economic Assessment of a 450 W Autonomous Photovoltaic System with Lithium Iron Phosphate Battery Storage

João Carriço[1], João Fernandes[2], Carlos Fernandes[3], Paulo Branco[*4]

[1]Department of Electrical and Computer Engineering, Instituto Superior Técnico, Universidade de Lisboa, Av. Rovisco Pais, 1, Lisbon, Portugal
e-mail: joao.carrico@tecnico.ulisboa.pt

[2]Department of Electrical and Computer Engineering, IDMEC, Instituto Superior Técnico, Universidade de Lisboa, Av. Rovisco Pais, 1, Lisbon, Portugal
e-mail: joao.f.p.fernandes@tecnico.ulisboa.pt

[3]Department of Electrical and Computer Engineering, IT, Instituto Superior Técnico, Universidade de Lisboa, Av. Rovisco Pais, 1, Lisbon, Portugal
e-mail: ffernandes@tecnico.ulisboa.pt

[4]Department of Electrical and Computer Engineering, IDMEC, Instituto Superior Técnico, Universidade de Lisboa, Av. Rovisco Pais, 1, Lisbon, Portugal
e-mail: pbranco@tecnico.ulisboa.pt

Cite as: Carriço, J., Fernandes, J., Fernandes, C., Branco, P., Technical and Economic Assessment of a 450 W Autonomous Photovoltaic System with Lithium Iron Phosphate Battery Storage, J. sustain. dev. energy water environ. syst., 6(1), pp 129-149, 2018, DOI: https://doi.org/10.13044/j.sdewes.d5.0191

ABSTRACT

This paper presents a study about an autonomous photovoltaic system making use of the novel Lithium Iron Phosphate as a battery pack for isolated rural houses. More particularly, this paper examines the behavior and efficiency of a low-cost isolated photovoltaic system for typical rural houses near Luena in Angola. The proposed system (solar panel, batteries, controller, and inverter) has been projected having in mind the required household daily load of 1,300 Wh and available solar irradiance. The initial batteries charging revealed to be essential to not only ensure a long battery life but using a balanced pack it was possible to achieve more stored energy. On-site, the polycrystalline solar panels used showed a daily average efficiency of 10.8%, with the total system having 75% efficiency. This result was adjusted to the average temperature in Angola. This way, it was made an extrapolation to the monthly irradiation values in Angola. The results achieved showed good energy production during almost all year except January and December, which revealed critical production values of 1,356 Wh and 1,311 Wh, respectively. These values are too close to the daily consumed energy and indicate the addition of a 2nd alternative source of energy (wind generator, diesel generator, etc.) to be explored further.

KEYWORDS

Angola, Autonomous/Off-grid photovoltaic system, System efficiency, Lithium iron phosphate battery.

INTRODUCTION

Electrical energy is a fundamental need for the economic growth and well-being of a developing society. Particularly, basic human needs demand electricity for household

* Corresponding author

usages such as refrigeration and lightning. As shown in a 2010 background paper of the World Bank Group energy sector strategy [1], it was estimated that in 2008 nearly 1.5 billion people had no access to electricity. Some 35% of those without electricity live in rural areas, mainly in North and Sub-Saharan Africa. From these, the International Energy Agency has estimated in 2009 [2] Burkina Faso, the Democratic Republic of Congo, Malawi, Mozambique, Tanzania and Uganda were among the countries with a rural access rate below 5%.

In [3], Tanzania and Mozambique were studied concerning the most important drivers and barriers for their rural electrification. The main driver found was political priority supported by government campaigns and programs. However, barriers as a strong dependency on foreign supporters and country's institutional disorganization were identified. More recently, a more specific study was made for Ghana [4]. Drivers were identified for electrification: economic structure, urbanization, income and energy prices. For these, Ghana population is inclined to pay between 7% and 15% of their salary to have a 24-hour supply of electricity. Hence, a complete removal of subsidies on electricity tariff in Ghana must be avoided. It would decrease significantly a household's electricity consumption, especially those with lower salaries.

In general, the Sub-Saharan Africa is the region most studied concerning rural electrification. A very recent review [5] points that scholars of this area see renewable energy technologies as the best option for remote regions far from the national grid on countries located in that area. The study also revealed that not only environmental and undoubtedly social benefits are implied, but off-grid solutions will be the most cost-competitive.

Different from previous studies that are focused at specific locations, a global approach to Africa's present and future power systems development is presented in [6]. Here, a set of electricity supply-demand scenarios-based models was employed to verify mainly the most efficient options and their cost-accessibility levels for African countries. Similar to the previous studies, the main conclusion was that all current energy policies implemented or in execution will take more than two decades to end energy poverty for only the Sub-Saharan Africa. The solution pointed out is to use Africa renewable energy resources because they are capable of providing faster access to electricity for all, particularly for the rural areas.

At this point, it is clear that for rural areas of developing African countries, the access to grid electricity continues to be very deficient. This happens once the distances involved are very large and until now do not justify the investment for supplying small populations. However, focus on rural electrification cannot wait because it aims to give people better-living conditions at low cost, with the certainty that there will be no short or medium term return, but those conditions will make all the difference in the development of the country. In this context, off-grid systems have been pointed out as the best solution.

Mandelli *et al.* [7] has systematized off-grid systems for rural electrification in five extents:

- Concerning the technology employed: layout and components;
- Models and methodologies for simulation and components sizing;
- Economic feasibility analyses;
- Case studies analyses.

In [8], a case study in Uganda looked for an optimum sizing methodology that could be applied to design an off-grid rural electrification system. That methodology was based on a solar Photovoltaic (PV) system plus a battery energy storage system that had to take into account not only the technical specificities but also economic costs in the medium term. Baurzhan *et al.* [9] proposes and tests a cost model that is also based on a similar solar PV plus batteries system but treating both cases for off- and on-grid situations. They show that, despite decreasing global costs in PV systems, in Sub-Sahara Africa costs

continue to be higher, mainly caused by the relatively high political and financial risks. Recent papers [10, 11] started to show that in terms of its better cost-benefit performance, it is today more logical to promote off-grid solar than grid-based electrification.

Financing off-grid electrification in Africa remains the real challenge today. Not only public funds need to be available, but also an economic and political atmosphere is needed for the creation of mainly private micro-finance groups. In this direction, Bhattacharyya [12] also concluded that it is urgent to remove investment barriers searching for collaborations, sharing different experiences. Some financing structures were proposed in [13] where the private sector is pointed as the main source of financing capital since public capital is still very limited for a fast development of African electrification.

Despite its huge natural resources (mostly hydro potential), Angola is a country put in in this context, with a per-capita energy consumption below the average in Africa. As shown in [14], despite the large investments in its power-generation capacity until 2009 (mainly from hydroelectric power), Angola continues to present a very unreliable power transmission and distribution grid to guarantee a robust and stable electrical connection. The power grid is still very limited supplying only the big cities. It is estimated that in Angola less than 20% of the population has access to energy [15] and the power grid is still very limited supplying only the main cities.

There are groups of diesel generators that run on local networks to supply industries located in remote places, with problems of continuous electricity supply. The prolonged drought has also affected the river flows, which in turn force electricity production to stop. Also, as stated in [16], the dependence of the price of diesel fuel and its transportation costs, which despite being relatively low compared with European countries, are continually growing due to the decrease of natural resource reserves.

Off-grid PV installations are the key for a future distributed generation in Africa [17], which will allow autonomy of a household at a low infrastructure cost. The full autonomy depends on the energy storage, its efficient management and control being the key to ensure a long operation period.

It is in this context that this paper designs and tests the behavior and efficiency of a low-cost isolated (autonomous, off-grid or stand-alone) PV system with the novel Lithium Iron Phosphate ($LiFePO_4$) battery storage, for the rural area near Luena in Angola. The system (solar panel, batteries, controller and inverter) is designed having in mind the required household load and solar energy available. These determine the sizing of the PV panels' nominal power, $LiFePO_4$ battery pack storage capacity, the energy monitoring system, as well as the power of the inverter.

The main points studied in this paper can be summarized as:

- Definition of the energy pathways in an autonomous photovoltaic home system (recognition of the involved elements);
- Identification of the typical consumers profiles on a small residential building in Angola. Based on this, projection of the nominal values of each element that constitutes the system regarding the typical rural consumer profile;
- Cost-benefit analysis of the system in the study by verification and analysis of total experimental system efficiency results;
- Study and test of the behavior of the novel $LiFePO_4$ batteries under load when used in a group as a battery pack.

METHODS

Autonomous PV systems with battery energy storage are constituted by a string of PV panels, a solar regulator/controller to monitor the batteries' voltage levels and the battery pack. The energy produced by the PV panels is delivered to the loads, and the surplus

energy is stored in the batteries. The stored energy may be used during the night when there is no solar radiation. Consequently, the batteries must have enough capacity to feed the load during the night and/or on low solar radiation days. The regulator has the ability to cut-off the PV and also cut-off the consumers supply according to the battery voltage levels. While the use of Direct Current (DC) loads may avoid the use of an inverter, its efficiency and consumption in standby reduce the amount of available power to the loads. However, the use of DC loads is not very common and this equipment is always more expensive than Alternating Current (AC) equipment.

Two configurations are possible: connect the inverter to the solar regulator (Figure 1a) or directly to the batteries (Figure 1b). The use of an off-grid inverter is required when using AC loads. Solar regulators are usually projected for currents up to 50 A. Therefore, in case of loads without high current peaks, the inverter can be connected to the solar regulator as shown in Figure 1b. However, using a Battery Management System (BMS) commanding and monitoring the batteries as shown in Figure 1c, the PV system becomes more reliable and economical. In Figure 1c, the straight lines represent a direct connection and the dashed lines the control unit. The PV panels and the inverter operate at the rated voltage of the batteries and the BMS monitors each cell or the whole battery pack electrical parameters. The BMS actuates the relays opening and closing the circuit if the batteries go over or undercharging. The inverter has also its own protection like short-circuiting, under and over voltage, however, it should be ensured that the inverter and BMS actuation voltages do not conflict.

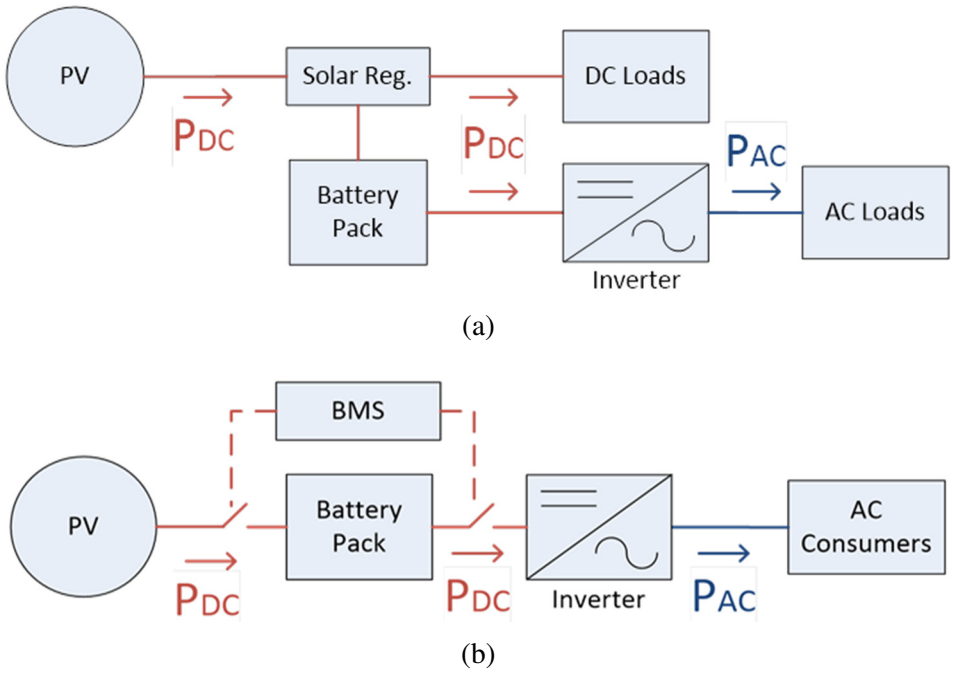

Figure 1. Block diagrams of different autonomous PV systems: an inverter connected to the solar regulator (a); inverter connected to the battery (b)

The AC loads are usually constituted by electrical motors, lights, TVs and other equipment with high starting currents that produce prohibitive currents on the DC side. These peaks may reach 100 A in the battery pack and go through the solar regulator. To avoid such currents in the regulator, a direct connection of the inverter to the batteries is a possible solution, as shown Figure 1b. Using this configuration, the regulator may connect/disconnect the PV panels and the DC loads. The inverter acts as a regulator, being the under-voltage protection for the batteries and thus disconnecting the AC loads. In this case, the efficiency of the inverter has to be taken into account because it might be

working at 20% of its nominal power since an oversizing of inverter rated power is necessary due to power peaks. The choice between the two different typologies (Figure 1) will thus depend on the cut off parameters of the inverter and also of regulator rated current.

There are several possible processes to project an autonomous PV system. Processes differ in the initial condition that will affect the design of the remaining components:

- Maximum daily energy calculation;
- Maximum power consumption calculation;
- Number of PV modules calculation;
- Battery capacity calculation.

To scale a PV system it is necessary to know the average radiation values at the installation site. To determine these values radiation PVGIS software was used. This software allows to estimate online the PV solar energy for isolated or grid-tied systems within the European and African continent and uses Google Maps® to choose the location.

The maximum daily energy calculation process must consider the following steps:

- Determine the daily energy consumed by the loads;
- Calculate the energy production of the PV modules at a given tilt (β) and azimuth angle (γ);
- Estimate the peak power of the PV modules;
- Calculation of the battery parameters;
- Selection of the solar regulator;
- Selection of the autonomous or off-grid inverter.

Battery Management System

The BMS is the solar regulator in Figure 1c, used to monitor the battery pack. The straight lines represent a direct connection and the dashed lines the control ones.

The most important feature in any application is to ensure no battery damage. A BMS is an electronic monitor device which controls the status of individual cells and pack. In order to protect and maximize battery pack's lifetime, the cell temperature, voltage and current are measured. To provide a better performance, the State of Charge (SoC) and eventually the State of Health (SoH) are estimated and different balancing strategies can be used depending on the system application. They are usually bottom or top balancing as it will be further analyzed in more detail.

The BMS actuates the relays opening and closing the circuit if the batteries go over or under the safe ranges of temperature, voltage and SoC ranges.

Lithium Iron Phosphate batteries

Energy production is the basis for the working time capacity of an autonomous system which additionally requires energy storing, in other words, batteries. Within the range of available chemical types, lithium type has high electrochemical potential which makes it one of the most reactive of metals. These properties give lithium the potential to achieve very high energy and power densities in many applications such as automotive and PV.

$LiFePO_4$ have some advantages compared with other lithium battery types but some working constraints. Lithium cells tend to have a different SoC when used in groups (connected in series or parallel) and submitted to several charge/discharge cycles. Enumerating some of the reasons, this could happen due to external temperature differences, cell's impedance differences or capacity manufacturing differences. The SoC of each cell individually is not detected by any SoC measuring instruments. As pointed in [18], the strategy to have the SoCs as close as possible is to do what is called balancing which should always depend on system application and is generally

done by a BMS. Protecting a single cell has a certain complexity, protecting a battery (a series string) is harder [19], cell voltages do not divide equally, temperatures vary, etc. The higher the protection, the higher the system cost, for this reason, the project is a balance between costs and capabilities as usual.

In summary, batteries used in autonomous PV systems must have reduced maintenance, long service time, reduced self-discharge and high energy efficiency, high storage capacity and power density, good performance/price relation, and protection against the occurrence of hazards to the environment and health. $LiFePO_4$ has the best thermal stability compared with Lithium Cobalt Oxide ($LiCoO_2$), Lithium Ion Manganese Oxide ($LiMn_2O_4$), Lithium Nickel Cobalt Aluminium Oxide ($LiNi_XCo_XAl_YO_2$) types, being thus appropriate to photovoltaic applications [20]. Regarding the charging/discharging characteristic in Figure 2, the main conditions that should be verified for $LiFePO_4$ batteries are:

- The voltage of the cell should not exceed 3.65 V when charging and 2.5 V when discharging. In Figure 2, OCV is the Open Circuit Voltage of the battery;
- The lifetime of the cells will be drastically reduced if charged outside the range 0 °C ~ 40 °C and discharged outside the range –20 °C ~ 60 °C;
- Cell's lifetime will be reduced if charged/discharged at current rate higher than 30% of the capacity (0.3 C).

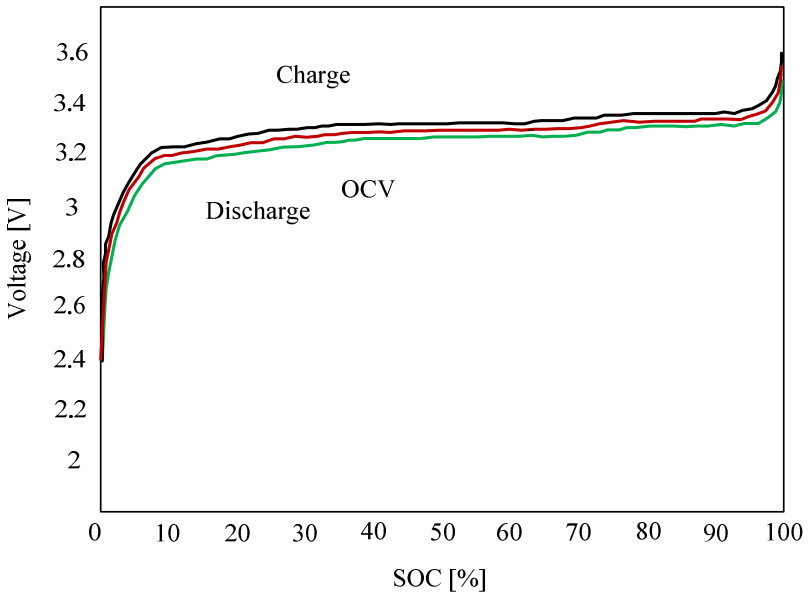

Figure 2. $LiFePO_4$ typical curves [7]

To estimate the batteries' SoC the Coulomb counting technique may be used, which simply indicates the remaining capacity of the battery by using electric current integration according to the coulomb counting equation [21] as follows:

$$\mathrm{SoC}_t = \mathrm{SoC}_0 - \int_0^t \frac{\eta \times i(t)}{C_\mathrm{n}} dt \quad (1)$$

Parameter SoC_0 is the initial SoC, η is the Coulomb efficiency, C_n is the battery estimated capacity and $i(t)$ is the current. The Coulomb counting is usually combined with other sensors, such as voltmeters to measure the battery voltage and calibrate the SoC to improve the lack of precision of the current sensors. Cells usually have slightly different capacities, for this reason the cell with the smallest capacity dictates the capacity of all the battery pack [20].

Another important fact to consider is that new lithium iron phosphate batteries are usually partially charged from the factory but due to transport, climate and environment conditions, the cells' SoC are different at the moment of assembling. When assembling the cells in a series string it is necessary to balance them so they can have a similar charging/discharging profile.

Off-grid inverter

For any PV system, the off-grid inverter is the essential electronic device that converts low voltage DC from the battery to the 100 V-120 V or 220 V-240 V AC signal from the grid. Pure sine wave inverters have a Total Harmonic Distortion (THD) lower than 3% which was confirmed experimentally. The efficiency of the inverter is obtained as follows:

$$\eta_{\text{inv}} = \frac{P_{\text{OUT}}}{P_{\text{IN}}} = \frac{P_{\text{AC}}}{P_{\text{DC}}}[\%] \tag{2}$$

Figure 3 shows in advance† the typical experimental characteristic of a 1,500 W pure sine wave off-grid inverter. The curved plots its efficiency for different loads. The efficiency ranged from 84-90% between 200-300 W (peak load of 250 W) with the highest value at 800 W (50% of the nominal).

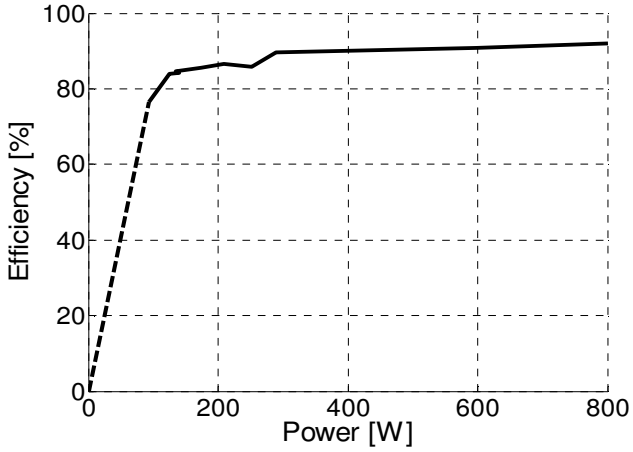

Figure 3. Typical off-grid inverter characteristic with a purely resistive load

Angola case-study

The case study presented in this section is Angola – a country on the west coast of Africa in a tropical zone in the latitude range of 6 to 17°S and 12 to 23°E longitude range. More particularly, the rural interior zone of Luena at 11° 47' 31.3"S and 19° 54' 30.1"E is studied in more detail.

Angola is a country with a large energy gap, 250 kWh/per capita, which places it behind the average per-capita consumption in Africa. According to the Angolan ministry of energy and water, there is a need for implementation of solar photovoltaic systems in rural zones, for electrification of social infrastructure, including schools, medical centers and administrative buildings.

In Angola, the global solar irradiation is above 2,000 kWh/m²/year, especially in the interior and south areas. Table 1 represents the averages irradiances at the horizontal (GHI) (kWh/m^2/year) and Tilted plane (GTI) (kWh/m^2/day). Term D/G is the annual ratio of the total radiation arriving at the ground which is due to diffuse radiation.

† The inverter was tested during the experimental run

Variables GTI and GHI are the most important radiations to projects using PV panels and when tilted to the optimum angle some annual mean gains may be observed relative to the horizontal position. For this reason, GTI_{opt} is the radiation value to be considered.

Table 1. Average annual GHI, GTI_{opt} and D/G in some Angolan cities (source: http://re.jrc.ec.europa.eu/pvgis/imaps/index.htm)

Location	GHI [kWh/m²/day]	GTI_{opt} [kWh/m²/day]	D/G
Luanda	5,600	5,650	0.38
Luena	5,870	6,100	0.33
Huambo	5,870	6,120	0.33
Lubango	6,070	6,360	0.29
Namibe	6,370	6,540	0.28

Regarding Angola climate characteristics, Figure 4 represents the daily average GHI and GTI_{opt} (irradiation) for each month in Luena city. According to this database, the optimal inclination for Luena area is 19 degrees (annual mean).

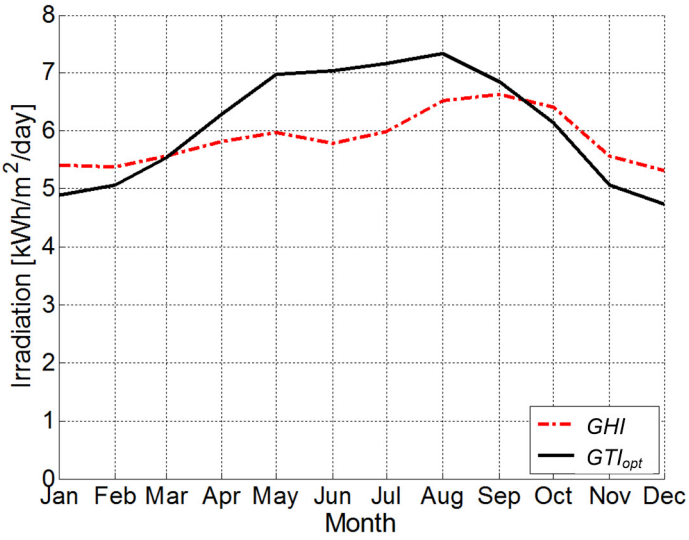

Figure 4. Daily mean solar radiation values in Luena, Angola (source: PVGIS Climate-SAF database 2001-2012)

Luena registered the lowest values in the rainy season from November to March and the highest in the dry season from April to October. This result goes in line with the rest of the country. The annual GHI average is 5,870 Wh/m²/day and the GTI_{opt} is 6,100 Wh/m²/day resulting in a gain of 3.92% at the optimally inclined plane.

Temperature and sunshine hours. The geographical position of Angola provides a radiation of 10 to 12 hours per day during the entire year. Table 2 lists some annual mean climate conditions for Angola region. The annual mean sunshine hours range from 2,200 to about 2,400 hours and the mean temperatures from 19 to 25 °C.

Table 2. Average annual GHI, GTI_{opt} and D/G in some Angolan cities (source: http://re.jrc.ec.europa.eu/pvgis/imaps/index.htm)

Location	Alt. [m]	Climate	Min/av/max temp. [°C]	Sunshine [h]
Luanda	74	Subtropical thorn woodland	22/25/28	2,340
Luena	1,357	Subtropical moist forest	14/21/28	2,464
Huambo	1,700	Subtropical moist forest	12/19/26	2,401
Namibe	44	Subtropical desert	17/21/33	2,230

The dry season has more than 260 hours of sunshine per month and the rainy season reduces to 150-160 hours. The monthly average temperatures in Luena, Angola are represented in Figure 5. The lower temperatures are registered in the dry season between May and September (T_{min} = 9 °C, Ti_{med} = 18 °C, T_{max} = 26 °C). The higher temperatures between September and March occur at the cloudy season when the days are longer.

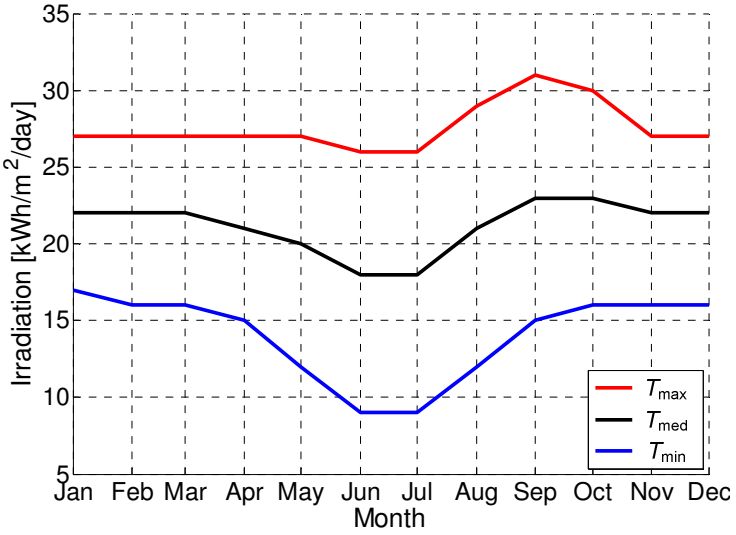

Figure 5. Average temperatures in Luena, Angola

Rural house characteristics and load. In this work, the considered electrical load for a standard rural house in Angola is shown in Table 3. To proceed with the future sizing, the average hours of utilization of each load was estimated. The refrigerator has a particular way of working, on an on-off regime, which makes it more difficult to know the corresponding utilization time at full load. For this reason, the energy consumption of a typical refrigerator was measured in the laboratory.

Table 3. Electrical loads for a standard house in Angola

Device	Nominal power [W]	Utilization hours [h]
Refrigerator	100	4-7
CRT TV 13''	40	2
Incandescent lamps	60	5

To perform a more accurate project, one replica of the rural house electrical consumers was done in the laboratory. The active power and power factor of each load were obtained and are presented in Table 4.

Due to the ON and OFF duty cycle of the refrigerator its energy consumption was measured during a 24 h period. The refrigerator has 7 refrigeration levels, consuming more energy for higher levels. Once it was not possible to simulate a diary use of the refrigerator, the level 4 was chosen, instead of the typical level 3, to compensate the extra consumption caused by the opening of the door on level 3.

Table 4. Electrical loads experimental power of standard house in Angola

Device	Nominal power [W]	Active power [W]	Power factor
Refrigerator	100	127	0.6
CRT TV 13''	40	41	0.674
Incandescent lamps	60	69.6	1

Figure 6 shows the average active power consumption of the refrigerator for a period of 1 h at level 4 without opening of its door. In each hour, the refrigerator compressor is active during four periods, each one of 4 minutes, at an average power of 127 W. The power peaks occur when the compressor motor starts which will have to be supported by the inverter. The total load diagram presented in Figure 7 shows the total power consumption of the three previous loads for one day.

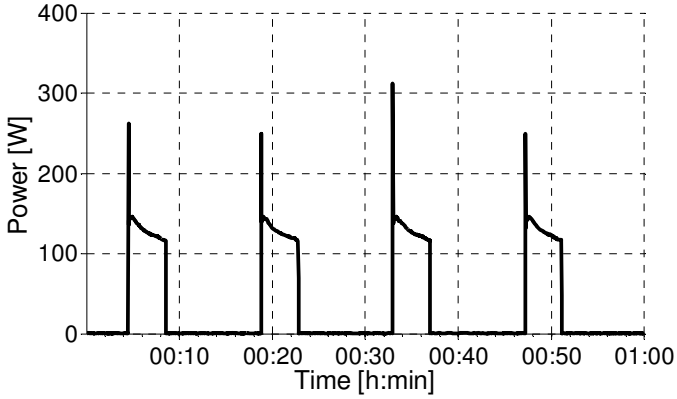

Figure 6. Refrigerator load diagram (1 h) of the KENT 201E model

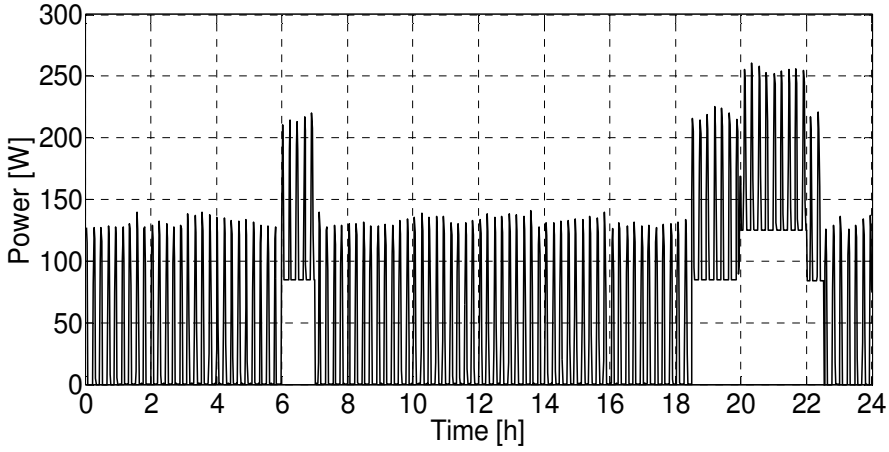

Figure 7. Loads diagram for a standard house in Angola

The lights turn ON between 6:00 and 7:00 and from 18:30 to 22:30 according to the hours before and after work in Angola. For a rural house it is estimated a 40 W TV, or equivalent device, working for 2 hours a day from 20:00 to 22:00. The maximum power of the system is 250 W between 20:00 and 22:00.

For the considered loads, their experimental daily energy consumption and hours of use are presented in Table 5.

Table 5. Experimental loads energy consumption

Device	Active power [W]	Utilization [h/day]	Daily energy [Wh/day]
Refrigerator	127	6.9	880
CRT TV 13''	41	2.05	84
Incandescent lamps	69.6	5	348
Total	237.6	5.52	1,312

The total daily consumption is approximately 1,300 Wh which should be taken into consideration for the project. The use of individual loads independently is equivalent to a

power of 238 W for 5.5 hours. Therefore the electrical consumers are characterized by a daily energy consumption of 1,312 Wh and a peak power of 250 W.

Experimental set-up

The sun's trajectory in the installation site can be obtained using SunEarth Tools software [22]. At last, the optimal angle to be considered to any installation site in Portugal can be estimated to be 35 degrees indicated in [23].

The autonomous PV system essays were performed in March 2015 with two polycrystalline 225 W panels installed on top of the third floor of North tower building at Instituto Superior Técnico (IST) (38° 44' 15.9"N and 9° 08' 17.6"W). The approximate sun's trajectory is shown in Figure 8. The solar maximum angle is 48° at 13:00, as indicated using SunEarth Tools. The panels are oriented to the geographical south (7° deviation from south to the west) with an inclination angle of $\beta = 35°$ (optimal angle generally used in Portugal).

The efficiency of the solar panel may be estimated knowing the temperature of the cells. Better results for the efficiency are produced if taking into account the temperature of the cells (T_c) and can be obtained experimentally using eq. (3), where η_{STC} is the efficiency of the panels at Standard Test Conditions (STC) conditions and γ approximately –0.004/K for polycrystalline silicon cells:

$$\eta(T) = \eta_{STC}[1 + \gamma(T_c - T_{STC})] \quad (3)$$

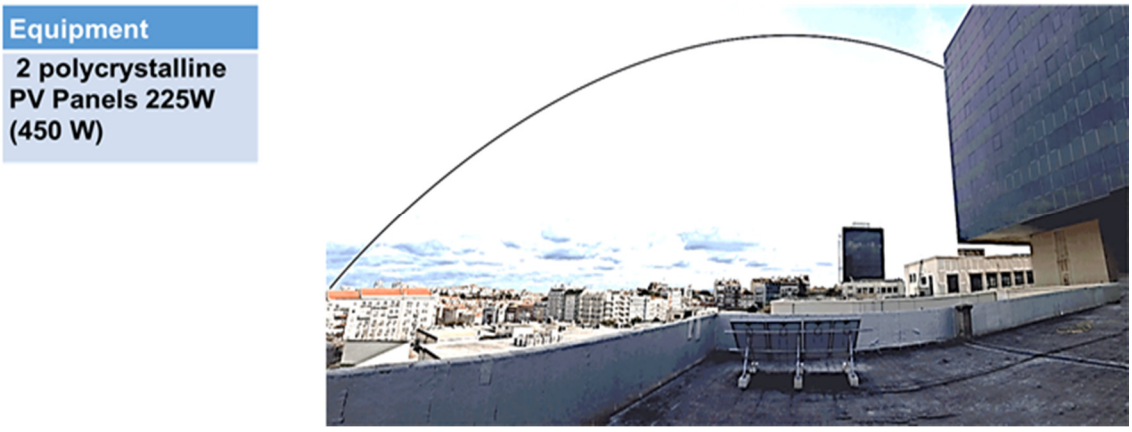

Figure 8. PV installation site at IST and sun trajectory in March

Due to logistic problems, the PV panels were obliged to be mounted at roof's department (Figure 8 shows its location) where they are shaded only before 8:30 and after 14:30. This is caused by the building height (morning) and by the north tower building (located right on the image of Figure 6), which reduces the solar radiation by at least 3 hours/day (afternoon). In the next plots, this shading effect will be indicated by a grey shadow area below the graphic.

Figure 9 shows the major components of the experimental arrangement installed in the laboratory. The battery pack is installed at the bottom of the experimental bench (Figure 9a) and is connected to a relay in series (item 5 on Figure 9b), controlled by the BMS controller (item 6). The relay is connected to the PV panels and the inverter main circuit (item 4). The BMS uses a current sensor (item 7) to measure the current going in and out of the battery pack. The PV panel's circuit is protected by a 25 A DC fuse (item 2) and may be manually switched on/off by a DC switch (item 3). Also visible in Figure 9b are the data acquisition devices that perform data logging of the voltages of the system (item 1).

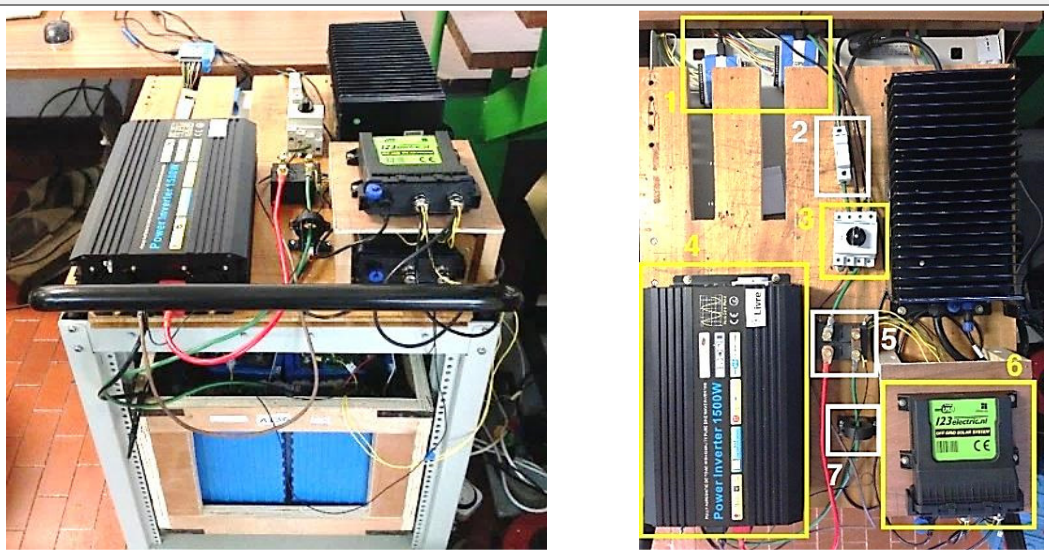

(a) (b)

Figure 9. The experimental set-up of the autonomous PV/battery storage system: complete system view (a); up view with all elements numbered (b)

Batteries

Usually, the nominal operating voltage of the PV system can choose between 12 V, 24 V or 48 V. The working voltage chosen was 24 V instead of 12 V to decrease the current on the cable and consequently the losses. The daily consumption in Ah is given by eq. (4) which results in 54.17 Ah for U_{DC} = 24 V. The battery sizing was computed as in eq. (5), where N_D is the number of reserve days (working days without sun). DOD_{max} is the maximum deeph of discharge of the battery which should be less than 80% so the batteries can perform more than 2,000 cycles. The results give a 169.28 Ah battery bank with the reserve days equal to 2.5:

$$W_{\mathrm{Ah}} = \frac{W_{\mathrm{D}}}{U_{\mathrm{DC}}}\,[\mathrm{Ah}] \tag{4}$$

$$C_{\mathrm{BAT,Tot}} = \frac{W_{\mathrm{Ah}} \times N_{\mathrm{D}}}{\mathrm{DOD}_{\mathrm{max}}}\,[\mathrm{Ah}] \tag{5}$$

Choosing a 180 Ah battery, the number of batteries needed is just one. The battery capacity is added when the batteries are installed in parallel keeping the voltage and remains the same when they are installed in series, adding to the voltage. In this case to perform the 24 V, more batteries are needed in fact. Due to the nominal voltage of 3.2 V of each $LiFePO_4$ battery, 8 batteries were necessary in order to obtain the 24 V system. Thus, in order to build a battery bank with 24 V and 169 Ah, eight batteries with 180 Ah and 3.2 V are needed.

Initial charging of the batteries. The influence of the initial charge (after leaving the factory) of all cells of a battery pack in the battery capacity was tested. Figure 10 illustrates a partial discharge test comparison between an unbalanced (Figure 10a) and balanced (Figure 10b) initial charge battery pack, on a constant resistive load of 6 Ω. For an ambient temperature of 15 °C and an initial voltage of 26.15 V, the two previous partial discharge tests were done, until the BMS detected a voltage of 2.7 V in one cell. Results are shown in Figure 10 for the unbalanced and balanced initial conditions. Additionally, in Table 6, the energy capacities are compared.

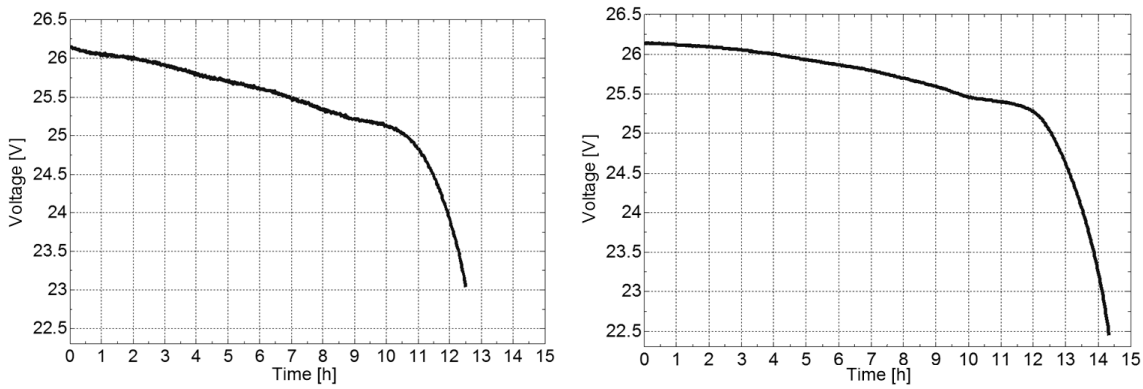

(a) (b)

Figure 10. Battery pack voltage during discharge on a constant resistive load of 6 Ω without (a); and with initial balancing (b)

Table 6. Energy of the discharge tests in Figure 10

Unbalanced cells energy [Wh]	Balanced cells energy [Wh]
1,351	1,539

The initial charging produced an energy improvement of 12%, a clear gain in the discharge time which suggests that the pack should be always charged before use.

Off-grid inverter

Choosing a slightly larger inverter could allow it to run cooler and can anticipate a future load expansion. To understand what is the peak power of the loads involved the transitory AC current of the inductive loads was measured. In Figure 11 is represented the starting and the operating current of the refrigerator.

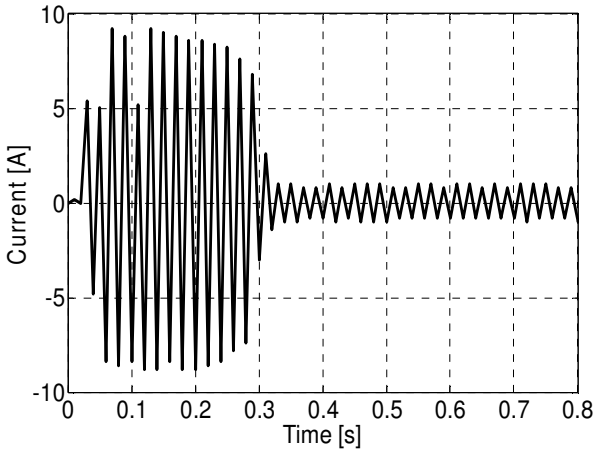

Figure 11. Refrigerator starting current

The peak amplitude of the current is I = 9.2 A, resulting in a peak power of about 1,500 W. Considering the general fact the inverter may support twice its nominal power for a small period, the minimum inverter power necessary is then 750 W.

The autonomous Photovoltaic/battery storage run – Lisbon, Portugal

Figure 12 shows in dotted-grey, the measured solar radiation on a horizontal surface on 14th March 2015 at the IST meteorological station, which is installed on the top of the

South Tower where the shading effect after 14:30 does not happen. The curve fluctuations represent the passing of clouds. It also shows in black, the radiation incident on the PV tilted plane (35°) calculated accordingly to the eq. (6) and Figure 13:

$$G_{\text{b\_module}} = \frac{G_{\text{b\_horiz}}}{\sin \alpha} \cos \theta_{\text{i}}(\beta) = \frac{G_{\text{b\_horiz}}}{\cos \theta_{\text{i}} \, (\beta = 0°)} \cos \theta_{\text{i}}(\beta) \tag{6}$$

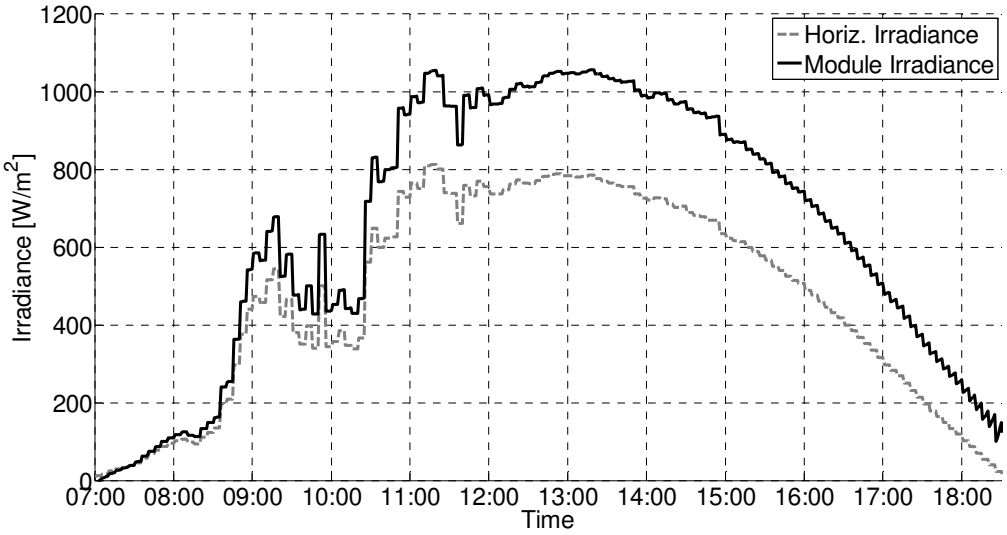

Figure 12. Total solar irradiance incident on a horizontal (dotted-grey) and 35° tilted plane (black) on 14th March 2015

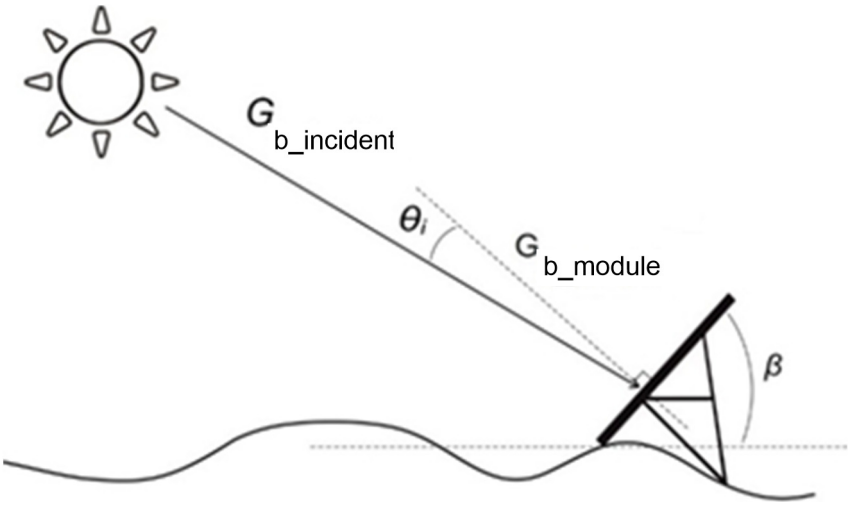

Figure 13. Solar rays on the referential of the PV panels

To simplify the calculations, the direct irradiance on the horizontal plane $G_{\text{b\_horiz}}$ was substituted by the total horizontal irradiance measured at the IST meteorological station once the diffuse radiation represents less than 10% of the total radiation.

The solar power is only injected into the batteries when the irradiance is available and voltage of the panels is higher than the voltage of the batteries. Figure 14 shows the evolution of the PV (black) and battery pack voltages (grey) during the day. The peaks seen on the graph after 14:00 represent the opening of the charging relay when the batteries are at full charge and voltage of one of the cells is above 3.5 V, remaining open for approximately 10 minutes. The profile of the loads influences the voltage of the batteries, mainly with the variations caused by the refrigerator.

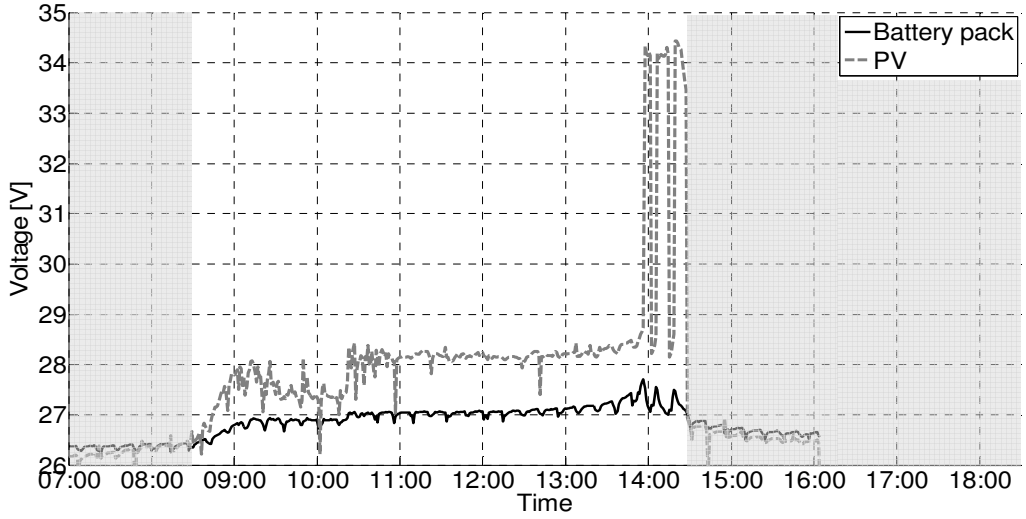

Figure 14. PV (black) and battery pack voltage (grey) on 14th March 2015

The refrigerator turns ON approximately every 15 minutes causing the battery voltage to drop. After 14:30 the panels are shadowed, providing no power, the loads being fed only by the batteries. The efficiency of the autonomous system (without the PV) was experimentally calculated accordingly to eq. (7), taking into account the period from 14:15 of the previous day (batteries fully charged) to the next day, with the system operating all day and night for the typical profile load in Figure 7. Typical values for the efficiency of the BMS (η_{BMS}), batteries (η_{BAT}), inverters (η_{inv}) and cable losses (η_{losses}) are shown in Table 7:

$$\eta_{\mathrm{syst,aut}} = \eta_{\mathrm{BMS}} \times \eta_{\mathrm{BAT}} \times \eta_{\mathrm{inv}} \times \eta_{\mathrm{losses}} \ [\%] \tag{7}$$

Table 7. Typical devices efficiencies

Device	Efficiency
BMS	98%
Batteries	> 99% (for I < 10%ln)
Inverter	85%-90%
Cables	97% (for typical lengths)
Total	About 81%

The charging of the battery pack was achieved in about 6 hours at 14:00. This charge state was used as the reference point for the estimation of the efficiency once the system took 23:45 h to discharge and charge again to the same voltage when the discharging was started. Table 8 summarises the energy of the main components of the system.

Table 8. Daily energy of the different components

PV production	Injected in battery	Load consume	Bat. + BMS + inverter losses
1,693 Wh	1,600 Wh	1,270 Wh	331 Wh

The losses on the DC cables added up to 93 Wh, 5% of the production, due to their long length (about 100 m from the rooftop to the laboratory). These values result in a mean daily efficiency of the system (cables + battery + BMS + inverter) of about 75% but can be improved to 80% if typical lengths of 10 m are considered for the cables. Figure 15

shows the influence of the ambient and the photovoltaic cell's temperature on the efficiency of the PV panels during its operation. Before analyzing the results, it is important to say that the manufacturer indicates 13.6% efficiency at STC.

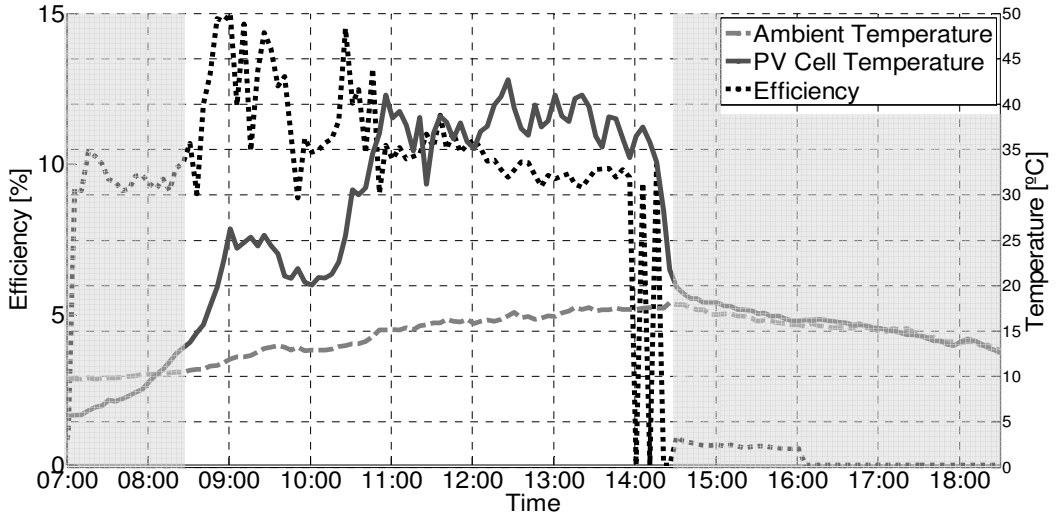

Figure 15. PV module temperature and efficiency on 14th March 2015

At the beginning of the day, the panels work mainly with diffuse and reflected radiation once the sun rays hit the panels close to 8:30 (shaded area) which makes an eq. (6) meaningless for this case.

When the radiation focuses the panels with a considerable irradiance (600 W/m²) its temperature increases considerably to 25 °C, the efficiency being 14.7% at 9:00. The increase of the efficiency verified at this time of the day is slightly higher than the efficiency of the manufacturer, once the clouds make the diffuse radiation component increase considerably. The diffuse component is summed to the direct component, increasing the total incident radiation for a cloudy test conditions study. This indicates that eq. (6) does not work properly for more than 10% diffuse radiation conditions. With clear sky after 11:00, the temperature of the cells increases to 40 °C, a consequence of the increase of the radiation and ambient temperature. The fluctuations of the panels' temperature are caused by the wind cooling effect. The average efficiency for the period between 8:30 and 14:00 is 10.8%.

The autonomous Photovoltaic/Battery storage run – Luena, Angola

Since it is not possible to make experimental tests in Angola, it is important to compare its radiation with the radiation in Portugal where the system was tested to assess its viability and efficiency. This way it is possible to make an extrapolation of the energy produced in Angola by correcting the real efficiency of the panels to the average ambient temperature in Angola. The annual average temperature in Luena is 21.2 °C as opposed to 16.3 °C in Lisbon (ΔT = 5 °C). The efficiency variation with ΔT = 5 °C is approximately −0.3% accordingly to eq. (1). Consequently, for the energy production estimation in Table 7, a PV efficiency of 10.5% is used (10.8% in Lisbon) and a system efficiency of 80%, as the system tested in Lisbon may be improved by 5% using shorter cables (less than 10 m). The irradiation values shown in Table 9 were obtained from [24] for an optimal inclination angle of 19°.

On an average basis, even with a higher average ambient temperature than in Portugal, and a consequent lower PV efficiency, the higher solar potential in Angola leads to satisfactory energy production results. Analysing Table 6, we might conclude that only January and December are critical with an energy delivered to the loads close to the

1,300 Wh daily domestic consumption. Additionally, the estimated percentage of days with fully discharged batteries is less than 5% for an autonomous PV system in Luena with the following parameters: PV power 450 W_p, battery voltage 24 V, capacity 130 Ah, discharge cut-off limit 35%, daily consumption 1,300 Wh, module inclination 19° and orientation north (180°). This establishes that Angola has a high solar potential.

Table 9. Estimated energy available to the loads in Luena, Angola [24]

Month	Irradiation [Wh/m²/day]	Energy on PV panels area [Wh/day]	PV production [Wh/day]	Energy available to the loads [Wh/day]
Jan.	4,890	16,137	1,694	1,356
Feb.	5,070	16,731	1,757	1,405
Mar.	5,540	18,282	1,920	1,536
Apr.	6,290	20,757	2,180	1,744
May	6,980	23,034	2,419	1,935
Jun.	7,040	23,232	2,439	1,952
Jul.	7,170	23,661	2,484	1,988
Aug.	7,330	24,189	2,540	2,032
Sept.	6,850	22,605	2,374	1,899
Oct.	6,150	20,295	2,131	1,705
Nov.	5,070	16,731	1,757	1,405
Dec.	4,730	15,609	1,639	1,311
Annual average	6,093	20,105	2,111	1,689

Prototype costs

The system was built considering the project and is specified in more detail in Table 10. The distance from the PV source to the batteries should be as low as possible which may reduce the system costs. Although the design capacity of the battery is approximately 180 Ah, at the time of purchase the highest capacity battery available at the supplier's store was 130 Ah.

Table 10. Total PV/battery storage system cost

Item	Units	Price with VAT (EUR)	Total (EUR)	Percentage of budget [%]
225 W polycrystalline PV panels	2	303	606	20.0
DC aluminium cable 4 mm^2	50 × 2 m	0.86 EUR/m	86	2.8
$LiFePO_4$ batteries 3.2 V 130 Ah	8	127.48	995.84	32.9
123 BMS + Controllable relay	1	490.58	490.58	16.2
BMS board cell module	8	11.06	88.48	2.9
DC current sensor 100 A	1	55.62	55.62	1.8
1,500 W off-grid inverter	1	528.9	528.9	17.5
DC switch	1	101	101	3.3
Dead front fuse holders	1	6.22	6.22	0.2
Differential circuit breaker I_n = 25 A, $I_{\Delta n}$ = 3 mA	1	68.2	68.2	2.3
Total			3,026.8	100

Thus the 130 Ah batteries were used for testing, reducing also the system costs that way. To perform better with motor loads, the inverter must support its peak power. In this case, the available inverter had a nominal power of 1,500 W, much higher than the required one (peak power 3,000 W). The total 450 W_p system cost corresponds to a price of 6.9 USD/W (6.3 EUR/W), inside the range of 2.7 to 20 USD/W reported by the

International Energy Agency Photovoltaic Power Systems for the off-grid sector (< 1 kW). The batteries with the BMS system correspond to half of the total cost.

DISCUSSION

On-site, the polycrystalline solar panels presented a daily average efficiency of 10.8% and the autonomous system a 75% efficiency that can be improved by about 5% if the panels are installed at a shorter distance (about 10 m) of the battery pack. The efficiency of the PV panels experimentally obtained in Portugal was adjusted to the average temperature in Angola so that it was made an extrapolation to the monthly irradiation values in Angola. The results showed a high energy production during almost all the year, except in January and December which revealed critical production values of 1,356 Wh and 1,311 Wh, respectively. These values being close to the daily consumed energy, the addition to the system of a 2nd alternative source of energy (wind generator, diesel generator, etc.) is suggested. Another possible solution to improve performance in the critical months is a manual change of the tilt angle of the panels in order to align them with the sun. Using a $\beta = 0°$ tilt angle the irradiation may be 10% higher according to PVGIS data.

The estimation method of direct solar radiation incident on the plane of the panels (G_{b_module}) calculated from experimental measurements of radiation in the horizontal plane on site (G_{b_horiz}), revealed a deviation of about 2.7% from the experimental value. This value shows that the procedure used for the calculation is suitable for clear sky days. However, this method has the limitation of not working properly when the solar angle is close to zero.

With respect to the batteries, the initial charging revealed to be essential to ensure a long life of the batteries and with a balanced pack, it is possible to increase the energy storage capacity to about 12%. The control systems showed to be also related to the performance of the batteries. These systems should consume the lowest power, as their use must reduce the battery energy capacity to supply the installed sensors. This fact will unbalance the batteries faster compared with a system without a battery management system. The Depth of Discharge should not exceed 80% of the full charge, since if the system is discharged for an extended period, BMS stand-by consumption, although small, can cause the cells to go below the minimum voltage. However, the implications of this idle power have not been verified experimentally once it would be necessary to measure the cells capacity after some years of operation. The standby power of ©BMS123 is less than 0.3 W (idle current < 10 mA). The control system had some limitations in reading the output currents of the batteries. Since the inverter voltage input signal is a square wave the current is not a constant DC value. This introduces small errors on the real SoC Coulomb counting estimation method which may lead the controller to open the circuit before the batteries are actually discharged. This may be fixed by calibrating the current sensor offset or ignoring the estimation of SoC that could make the system simpler and cheaper to implement. Nevertheless, the cells' protection is ensured once the relays open the circuit based on voltage signals which work properly.

On-site, the polycrystalline solar panels used showed a daily average efficiency of 10.8% and the total system a 75% efficiency which may be improved about 5%, if the panels are installed at a distance lower than 10 m of the battery pack.

CONCLUSIONS

This paper presents an autonomous PV energy supply system for a typical rural house in Angola with the novel $LiFePO_4$ batteries. One prototype of the system was built in the Instituto Superior Técnico in Lisbon, Portugal, in order to be able to draw conclusions about its performance and cost and extrapolate its results to the rural consumers in

Angola. From the experimental results, it was concluded that the system would need to be capable of feeding the previous typical rural consumers with an average consumption of 1,300 Wh/day.

The experimental tests performed revealed good results for the projected system, the correct charging of the batteries and feed of the loads every day making the PV system work for the consumer's daily needs, even with the shadow constraint at the installation site.

The consumer's energy requires a minimum PV production of 1,625 Wh/day, the excess produced energy charges the batteries. The panels showed an efficiency of 10.8% and the system battery + BMS + inverter an efficiency of 80%. The number of reserve days of the system is up to two days which gives a good chance to the batteries charge again in a place with good sunshine index.

The batteries should be installed in a place as cool as possible to achieve the best batteries' capacity performance. Portugal has more constraints in the winter than Angola during the rainy season due to Angola's higher solar potential. Both sites require the panel's inclination angle adjustment during the less favorable months to reduce the risk of system shutdown.

This paper shows that the cost of this system, 6.9 USD/W, is in the lower range of off-grid solar autonomous systems used in Europe (2.7 to 20 USD/W). It is expected to open new opportunities for further investigations which may improve with more detailed methods of operation of these systems.

ACKNOWLEDGMENT

This work was supported by national funds through the Fundação para a Ciência e a Tecnologia (FCT) of the Portuguese Government with reference UID/EEA/50008/2013 and also supported by FCT, through IDMEC, under LAETA project UID/EMS/50022/2013.

NOMENCLATURE

A	tilted surface azimuth angle	[deg]
A_{S}	solar azimuth angle	[deg]
C	cell capacity	[-]
E_{d}	daily energy required by the loads	[J]
G	solar irradiance	[W/m^2]
G_{b}	beam radiation	[-]
G_{d}	diffuse radiation	[-]
G_{global}	global radiation	[-]
G_{module}	module radiation or radiation incident on the tilted plane	[-]
$G_{\mathrm{b\_incident}}$	maximum incident (beam) radiation	[-]
G_{r}	reflected radiation	[-]
H_{h}	irradiation on horizontal plane	[Wh/m^2/day]
H_{i}	solar irradiation	[kWh/m^2]
H_{opt}	irradiation on optimally inclined plane	[Wh/m^2/day]
I_{pack}	current circulating in the battery pack	[A]
I_{RMS}	root mean square current	[A]
$P_{\mathrm{loads,peak}}$	peak power of the loads	[W]
$P_{\mathrm{inv\_min}}$	minimum inverter power	[W]
$U_{\mathrm{DC}} \equiv U_{\mathrm{BAT,Tot}}$	total battery direct current voltage	[V]
U_{RMS}	root mean square voltage	[V]

Greek letters

α	solar altitude or solar elevation angle	[deg]
β	surface inclination angle	[deg]
β_{opt}	optimal inclination angle	[deg]
η_{BAT}	battery efficiency	[%]
η_{BMS}	battery management system efficiency	[%]
η_{inv}	inverter efficiency	[%]
η_{PV}	photovoltaic panels efficiency	[%]
$\eta_{\text{syst,aut}}$	autonomous/off-grid system efficiency	[%]
θ_{i}	incidence angle	[deg]

REFERENCES

1. Crousillat, E., Hamilton, R. and Antmann, P., Addressing the Electricity Access Gap, Background Paper for the World Bank Group Energy Sector Strategy, 2010, http://siteresources.worldbank.org/EXTESC/Resources/Addressing_the_Electricity_Access_Gap.pdf, [Accessed: 05-November-2017]
2. Song, Wei-dong, Fang, T., Wang, Q. K. and Zhou, Y. B., Summary of the Key Points of IEA World Energy Outlook 2009, Energy Technology and Economics, 2010, http://www.worldenergyoutlook.org/media/weowebsite/2009/WEO2009.pdf, [Accessed: 05-November-2017]
3. Ahlborg, H. and Linus, H., Drivers and Barriers to Rural electrification in Tanzania and Mozambique-grid-extension, Off-grid, and Renewable Energy Technologies, *Renewable Energy*, Vol. 61, pp 117-124, 2014, https://doi.org/10.1016/j.renene.2012.09.057
4. Taale, F. and Christian K., Households' willingness to pay for reliable Electricity Services in Ghana, *Renewable and Sustainable Energy Reviews*, Vol. 62, pp 280-288, 2016, https://doi.org/10.1016/j.rser.2016.04.046
5. Trotter, P. A., McManus, M. C. and Roy M., Electricity planning and implementation in Sub-Saharan Africa: A Systematic Review, *Renewable and Sustainable Energy Reviews*, Vol. 74, pp 1189-1209, 2017, https://doi.org/10.1016/j.rser.2017.03.001
6. Ouedraogo, N. S., Modeling sustainable long-term Electricity Supply-demand in Africa, *Applied Energy*, Vol. 190, pp 1047-1067, 2017, https://doi.org/10.1016/j.apenergy.2016.12.162
7. Mandelli, S., Barbieri, J., Mereu, R. and Colombo, E., Off-grid Systems for Rural electrification in developing Countries: Definitions, Classification and a comprehensive Literature Review, *Renewable and Sustainable Energy Reviews*, Vol. 58, pp 1621-1646, 2016, https://doi.org/10.1016/j.rser.2015.12.338
8. Mandelli, S., Brivio, C., Colombo, E. and Merlo, M., A sizing Methodology based on Levelized Cost of Supplied and Lost Energy for Off-grid Rural Electrification Systems, *Renewable Energy*, Vol. 89, pp 475-488, 2016, https://doi.org/10.1016/j.renene.2015.12.032
9. Baurzhan, S. and Jenkins, G. P., Off-grid Solar PV: Is it an affordable or appropriate Solution for Rural Electrification in Sub-Saharan African Countries?, *Renewable and Sustainable Energy Reviews*, Vol. 60, pp 1405-1418, 2016, https://doi.org/10.1016/j.rser.2016.03.016
10. Jamal, N., Options for the Supply of Electricity to Rural Homes in South Africa, *Journal of Energy in Southern Africa*, Vol. 26, No. 3, pp 58-65, 2015, http://www.scielo.org.za/scielo.php?script=sci_arttext&pid=S1021-447X2015000300006
11. Peters, J. and Sievert, M., Impacts of Rural electrification revisited: The African Context, *Revue D'économie du Développement*, Vol. 23, pp 77-98, 2015, https://doi.org/10.1080/19439342.2016.1178320

12. Bhattacharyya, S. C., Financing Energy access and Off-grid electrification: A Review of Status, Options, and Challenges, *Renewable and Sustainable Energy Reviews*, Vol. 20, pp 462-472, 2013, https://doi.org/10.1016/j.rser.2012.12.008
13. Glemarec, Y., Financing Off-grid sustainable Energy access for the Poor, *Energy Policy*, Vol. 47, Supp. 1, pp 87-93, 2012, https://doi.org/10.1016/j.enpol.2012.03.032
14. Solarin, S. A. and Shahbaz, M., Trivariate causality between Economic growth, urbanisation and Electricity consumption in Angola: Cointegration and causality analysis, *Energy Policy*, Vol. 60, pp 876-884, 2013, https://doi.org/10.1016/j.enpol.2013.05.058
15. Angola Energy Report, Centre for Scientific Study and Research of Angola's Catholic University, Angola, 2011.
16. Bertheau, P., Cader, C., Huyskens, H. and Blechinger, P., The Influence of Diesel Fuel Subsidies and Taxes on the Potential for Solar-powered Hybrid Systems in Africa, *Resources*, Vol. 4, No. 3, pp 673-691, 2015, https://doi.org/10.3390/resources4030673
17. Mandelli, S. and Mereu, R., Distributed Generation for access to Electricity: "Off-main-grid" Systems from Home-based to Microgrid, *Renewable Energy for Unleashing Sustainable Development*, Springer International Publishing, pp 75-97, 2013, https://dx.doi.org/10.1007/978-3-319-00284-2_4
18. Arnold, G., Garche, J., Hemmer, S., Vogler, C. and Wohlfahrt-Mehrens, M., Fine-particle Lithium Iron Phosphate $LiFePO_4$ synthesized by a new Low-cost Aqueous Precipitation Technique, *Journal of Power Sources*, Vol. 119-121, pp 247-251, 2003, https://doi.org/10.1016/S0378-7753(03)00241-6
19. Xing, Y., He, W., Pecht, M. and Tsui, K. L., State of charge estimation of Lithium-ion Batteries using the Open-circuit Voltage at various Ambient Temperatures, *Applied Energy*, Vol. 113, pp 106-115, 2014, https://doi.org/10.1016/j.apenergy.2013.07.008
20. Andrea, D., Battery Management Systems for Large Lithium-Ion Battery Packs, Artech House, 2010.
21. Khan, M. R., Mulder, G. and Mierlo, J. V., An Online Framework for State of charge determination of Battery Systems using combined System identification approach, *Journal of Power Sources*, Vol. 246, pp 629-641, 2014, https://doi.org/10.1016/j.jpowsour.2013.07.092
22. SunEarthTools.com, http://www.sunearthtools.com/dp/tools/pos_sun.php, [Accessed: 05-November-2017]
23. Hafez, A. Z., Soliman, A., El-Metwally, K. A. and Ismail, I. M., Tilt and Azimuth Angles in Solar Energy Applications – A Review, *Renewable and Sustainable Energy Reviews*, Vol. 77, pp 147-168, 2017, https://doi.org/10.1016/j.rser.2017.03.131
24. PVGIS Climate-SAF Database, Institute for Energy and Transport (IET), 2001-2012, http://re.jrc.ec.europa.eu/pvgis/imaps/index.htm, [Accessed: 05-November-2017]

Paper submitted: 23.01.2017
Paper revised: 05.11.2017
Paper accepted: 05.11.2017